J. KOSAE Vol. 23, No. E 1 (2007) pp. 29~38
Journal of Korean Society for Atmospheric Environment

Penetration Efficiency of Charged Particles in a Cylindrical Tube Connection with Electrical Voltage Difference

Dong Keun Song and Tae-Oh Kim*
School of Civil and Environmental Engineering, Kumoh National Institute of Technology, 1 Yangho-dong, Gumi, Gyeongbuk 730-701, Korea
(Received 8 May 2007, accepted 27 June 2007)

Abstract

A cylindrical tube connection that has a voltage difference and is separated electrically by an insulator was modelled. The penetration efficiencies of charged particles passing through the connector tube were investigated. Typically, as the particle size decreases and the applied voltage difference increases, the penetration efficiency decreases. To assess the effect of the electrode geometry, various lengths of electric insulator and aerosol flow rate with a fixed tube length and tube diameter were used when calculating penetration efficiencies. The comparison of penetration efficiencies for various electrode geometry setups suggests that the penetration efficiency can be described as a function of the product of applied voltage and electrical mobility of charged particles. The diffusion loss from this and previous studies are compared. Further, an explicit form for penetration efficiency is provided as a function of a new non-dimensional parameter, Es (= $Z_pV/U_{avg}W$); $P_{es}=0.2\cdot\exp(-Es/0.6342)+0.8\cdot\exp(-Es/4.7914)$.

Key words : Penetration efficiency, Electrostatic loss, Diffusion loss, Tube connection, Voltage difference

1. INTRODUCTION

The adverse effects of atmospheric aerosol particles on human health have attracted interest recently, due to the increased mortality caused by the ultrafine airborne particles. The total rate of nanoparticle deposition in the lung increases as particle size decreases, especially for particles less than 100 nm in diameter (Jaques and Kim, 2000; Schiller *et al.*, 1986; Wilson Jr *et al.*, 1985; Tu and Knutson, 1984). Further, nanoparticles are more toxic to biological systems than larger particles of the same material (Vincent and Clement, 2000; Wichmann and Peters, 2000; Oberdörster *et al.*, 1995; Oberdörster *et al.*, 1992). Particulate matter discharged from diesel engines also consists of a large number of nanoparticles and has strong unfavourable effects on the lung (Donaldson *et al.*, 1998; Kittelson, 1998).

To analyze atmospheric particles, it is necessary to use measurement systems that can measure wide size ranges of the ambient aerosols. Impactor type samplers are typically used for measuring wide size ranges of aerosol particles, but detailed particle sizing and real-time measurement have not been possible. Although an electrical low-pressure impactor (ELPI) was developed for the rapid measurement of a broad size distribution (0.028~10 μm; Keskinen *et al.*, 1992), the ability of ELPIs to mea-

* Corresponding author.
Tel : +82-54-478-7634, E-mail : tokim@kumoh.ac.kr

sure a detailed size distribution is limited. For the real-time measurement of a detailed size distribution, therefore, a differential mobility analyzer (DMA) is widely used to measure size distributions of atmospheric particles (Kim and Ahn, 2005; Bae *et al.*, 2003; Woo *et al.*, 2001) and particulate matter discharged from Diesel engines (Lee *et al.*, 2006; Park *et al.*, 2003). A long differential mobility analyzer (LDMA) was developed to extend the measurable particle size range by Myojo *et al.* (2001), and Shimada *et al.* (2005) developed an LDMA-FCE system by combining the LDMA and the FCE (Faraday Cup Electrometer) to overcome limitations in the use of a CNC (condensational nucleus counter). Song *et al.* (2006) also suggested, on the basis of numerical and experimental methods, that it is possible to use the LDMA for measuring nanoparticles.

When measuring the size distribution of atmospheric particles using a DMA, the electrical mobility distribution of particles is obtained, rather than the size distribution. Hence, the so-called reduction or inversion process must be used to derive the size distribution of atmospheric particles from the measured electrical mobility distribution. However, the electrical mobility distribution measured by DMA-CPC or DMA-FCE system is different from the size distribution of the airborne particles, due to the following: diffusional broadening during transport by Brownian diffusion, transport loss caused by inertial impaction, gravitational settling and interception in tube connections, and limitations in the efficiency of instruments for counting the number of particles (Collins *et al.*, 2004). Diffusional losses in particle sampling systems that contain bends and elbows were studied by Wang *et al.* (2002), the detection efficiency of a condensation particle counter was investigated by Petäjä *et al.* (2006) and the diffusional transfer function of DMA has been studied by numerous researchers (for further information, see Song *et al.*, 2005 and Song and Dhaniyala, 2007).

However, there is no report of any analysis of the phenomenon that electrostatic loss results in a decrease of the penetration of charged particles when they pass through a connection of cylindrical tubes whose electrical voltage differs. Kousaka *et al.* (1986) showed that sampling efficiency degrades as a result of the electric field differing on the electrode setup in the DMA sampling port and, by using experimental and numerical methods, compared the penetration efficiency obtained from two different types of electrode. Chen *et al.* (1998) reported that when an electrical insulator resides between connection tubes, the electrostatic loss of charged particles increases, but they did not provide a fundamental analysis of the effect. Zhang and Flagan (1996) also noted that the electrostatic loss caused by the distortion of an electrical force field in the vicinity of a DMA outlet depends only the electrode setup geometry, especially for the DMA measurements. This is because the applied voltage difference is determined in order to classify charged particles that have a given electrical mobility.

We here present a theoretical and numerical analysis of the effect of the electrode setup geometry on the penetration efficiency of charged particles in transport through a cylindrical tube connection that has an electrical voltage difference. The trajectory of charged particles was analyzed and penetration efficiencies for various cases are presented.

2. DESCRIPTION OF THE MODEL

Figure 1 shows a cylindrical tube connection that has an electrical voltage difference. Cylindrical tubes situated on each side of an electrical insulator play the role of electrodes. Charged particles in a sampled aerosol flow, Q_a, enter from the left side and move downstream. In the vicinity of the corner of each electrode, the electric field is distorted and has radial components of electric force, F_E, which make the charged particles move in a radial direction away from their straight trajectories. As the charged particles move to the cylinder wall and are deposited, their penetration efficiency decreases. This cylindrical tube connection has dimensions as follows: total length L, length of electrical insulator W, and inner diameter D_{tube} (=2R). The axisymmetric cylindrical coordinate system was employed to describe the geometry of the model and the trajectories

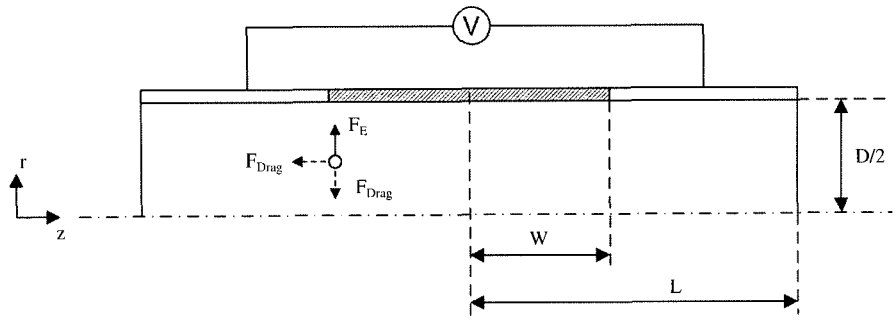

Fig. 1. Schematics of cylindrical tube connection with electrical voltage difference.

of the charged particles.

In the transport of airborne particles, gravitational settling, interception, inertial impaction, Brownian diffusion and acceleration by external forces are the principal mechanisms that affect particle behaviour. However, gravitational settling and interception are not considered, because the effects of those mechanisms constitute a very small portion of the overall effect and are not dominant in this case.

3. NUMERICAL METHODS

To obtain the penetration efficiency of charged particles in transport through a cylindrical tube connection that has an electrical voltage difference, (i) the flow velocity of air stream and electrical field strength are obtained by numerical methods in a 2-D cylindrical coordinate system, and (ii) the particle trajectories starting from the inlet of the tube with accounting electrostatic force exerting on charged particles and Brownian diffusion are calculated by using the Langevin equation. The resultant penetration efficiency is obtained from the final position of the charged particles in the tube.

3.1 Flow and electric field

Typical instruments for measuring particle size distribution are designed (i) to operate in laminar flow conditions and (ii) to avoid turbulent mixing (which deteriorates the performance of instruments) and change in particle characteristics (e.g., size distribution). Further, the sampled aerosol flow has fixed (steady) and low Mach number (incompressible) flow rates. Under these conditions, the flow inside this cylindrical tube connection can be assumed to be steady, incompressible and laminar. On the basis of the principle of the conservation of momentum, the incompressible Navier-Stokes equation (N-S equation) can be applied in this case. In this axisymmetric geometry and with the assumption $u_r(r, z)=0$, the radial component of the N-S equation vanishes and the axial component can be given by

$$\frac{1}{r}\frac{\partial}{\partial r}\left(r\frac{\partial u_z}{\partial r}\right)=\frac{1}{\mu}\frac{\partial p}{\partial r} \tag{1}$$

After integrating twice with boundary conditions, $u_z(r, z)=0$ at walls, the axial component of flow satisfies

$$u_z(r)=2U_{avg}\left[1-\left(\frac{r^2}{R}\right)\right] \tag{2}$$

where R is the radius of the tube connection and the average velocity in the tube $U_{avg}=Q_a/\pi R^2$.

The analytic descriptions of the electrostatic field are available for limited geometries; therefore, the electric potential and electrical forces are obtained by solving the Laplace equation numerically. The electrical potential V satisfies the Laplace equation and is given as an axisymmetric cylindrical coordinate system

$$\frac{\partial^2 V}{\partial r^2}+\frac{1}{r}\frac{\partial V}{\partial r}+\frac{\partial^2 V}{\partial z^2}=0 \tag{3}$$

Table 1. Boundary condition for electric potential.

$\frac{\partial V(R, z)}{\partial r}=0$	$-W<z<W$
$V(R, z)=V$	$-L\leq z<-W$
$V(R, z)=0$	$W<z\leq L$
$\frac{\partial V(r, z)}{\partial r}=0$	$r=0$
$\frac{\partial V(r, z)}{\partial z}=0$	inlet and outlet

with the boundary conditions given in Table 1.

3.2 Particle trajectory

In the calculation of the particle trajectories, particle-particle interactions, gravitational settling, and reaction between particle and gas are neglected; hence, the particle behaviour is described by only electrostatic forces, drag forces, and random motion caused by the collision of particles with gas molecules. The balance equation for forces acting on a charged particle is given as

$$m_p\frac{d\mathbf{v}}{dt}=\mathbf{F}-m_p\beta(\mathbf{v}-\mathbf{u})+\mathbf{X} \tag{4}$$

where m_p, β, $\mathbf{v}$ and $\mathbf{u}$ are the mass, friction constant, and velocity of the particle and gas stream, respectively. $\mathbf{F}$ and $\mathbf{X}$ are an external force and a random force, respectively. The friction constant of particles of diameter d_p is given by

$$\beta=\frac{3\pi\eta d_p}{m_p C_C} \tag{5}$$

where η and C_C are the gas viscosity and Cunningham's slip correction factor, respectively. Cunningham's slip correction factor, C_C, is a function of the particle Knudsen number, K_n ($=2\lambda/d_p$, where the λ is the mean free path of a gas molecule), given by (Allen and Raabe, 1982).

$$C_C=1+Kn[1.257+0.4\exp(-1.1/Kn)] \tag{6}$$

The Brownian diffusive motion of particles can be described by a random acceleration in the Langevin equation. The velocity and position of particles are determined by the values for the velocity and position at the previous time step, Δt, and the numerical schemes for calculating the velocity and position over time are provided in the literature (Song *et al.*, 2006; Song *et al.*, 2005; Ermak and Buckholz, 1980).

3.3 Penetration efficiency

The penetration efficiency of charged particles that is affected by electric force and Brownian diffusion in the cylindrical tube can be obtained by analyzing the final position of the simulated particles. For this calculation, a number of particles N_p started from the aerosol inlet. The particle number distribution is not uniform, because the axial velocity distribution over radial positions is parabolic, not uniform while the particle number concentration is uniform over radial positions. To consider the distribution of particle number concentrations at the aerosol inlet, the starting positions r_s of particles are determined by

$$\int_0^{r_s(k)} u_z(r)2\pi r dr=\left[\frac{2(k-1)+1}{2N_p}\right]Q_a,$$
$$\text{for } k=1, 2, ..., N_p. \tag{7}$$

The circular cross section is divided into (N_p-1) annular sections and one circular section (when k= 1). Here, N_p is the number of particle's starting positions. There may be particles that start from a radial position between those r_s positions. To simplify calculation, we assumed that all particles in k-th section start from the radial position, $r_s(k)$. The starting position of particles r_s represents particles in the annular section that enclose the corresponding starting position and the numbers of particles in each annular section are the same for all annular sections (Figure 2).

The resulting penetration efficiency, P, is obtained by dividing the number of particles that pass through the outlet of the cylindrical tube by the total number of particles that start from the aerosol inlet. If the particles collide with the walls of the tube connection, particles are assumed to stick on the wall and do not reenter the air stream. The particles that stick on the wall constitute the particle loss that occurs during transport through the tube connection.

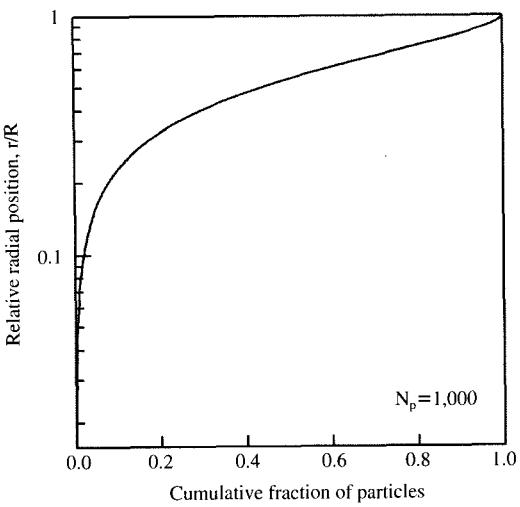

Fig. 2. Radial cumulative fraction profile of particle numbers over relative radial positions.

To obtain penetration efficiency with consideration of particle loss by electrostatic attraction and diffusion simultaneously, A hundred sets of numerical simulation were carried out.

4. RESULTS

The electrical potential V, which is described by the Laplace equation in 2-D cylindrical coordinates (r, z), was obtained by using numerical calculation (Finite Difference Methods) and a contour plot of the electrical potential when W/L=0.2 and the applied voltage difference is 100 V, is shown in Figure 3. The radial and axial components of the electrical strengths for the same case as Figure 3 are also shown in Figure 4 as contour plots. Although the

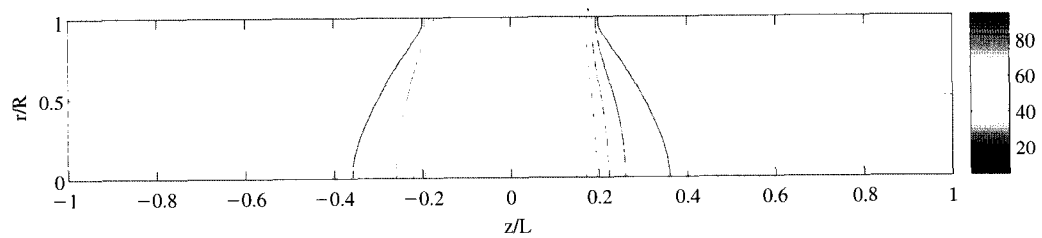

Fig. 3. Electrical potential when the applied voltage difference is 100 V and W/L=0.2.

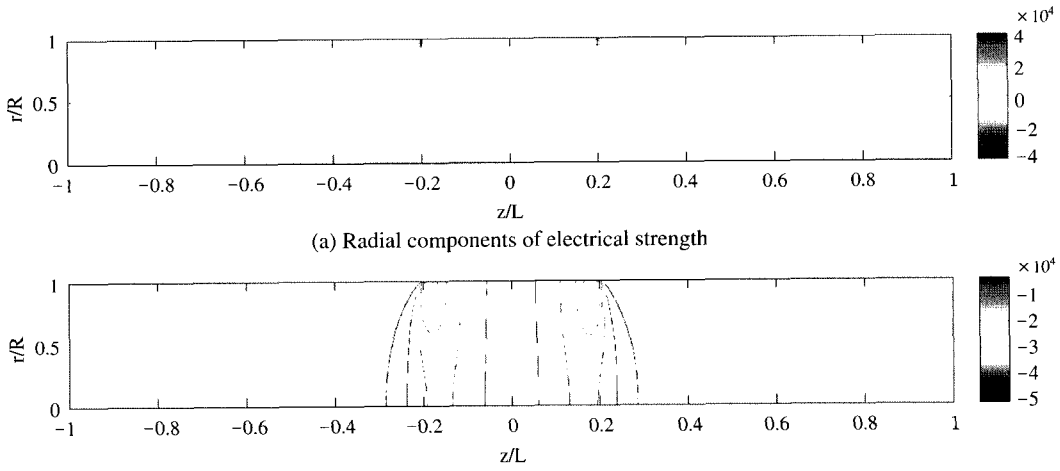

Fig. 4. Contour plot of radial (a) and axial (b) electric strengths when the applied voltage difference is 100 V and W/L=0.2.

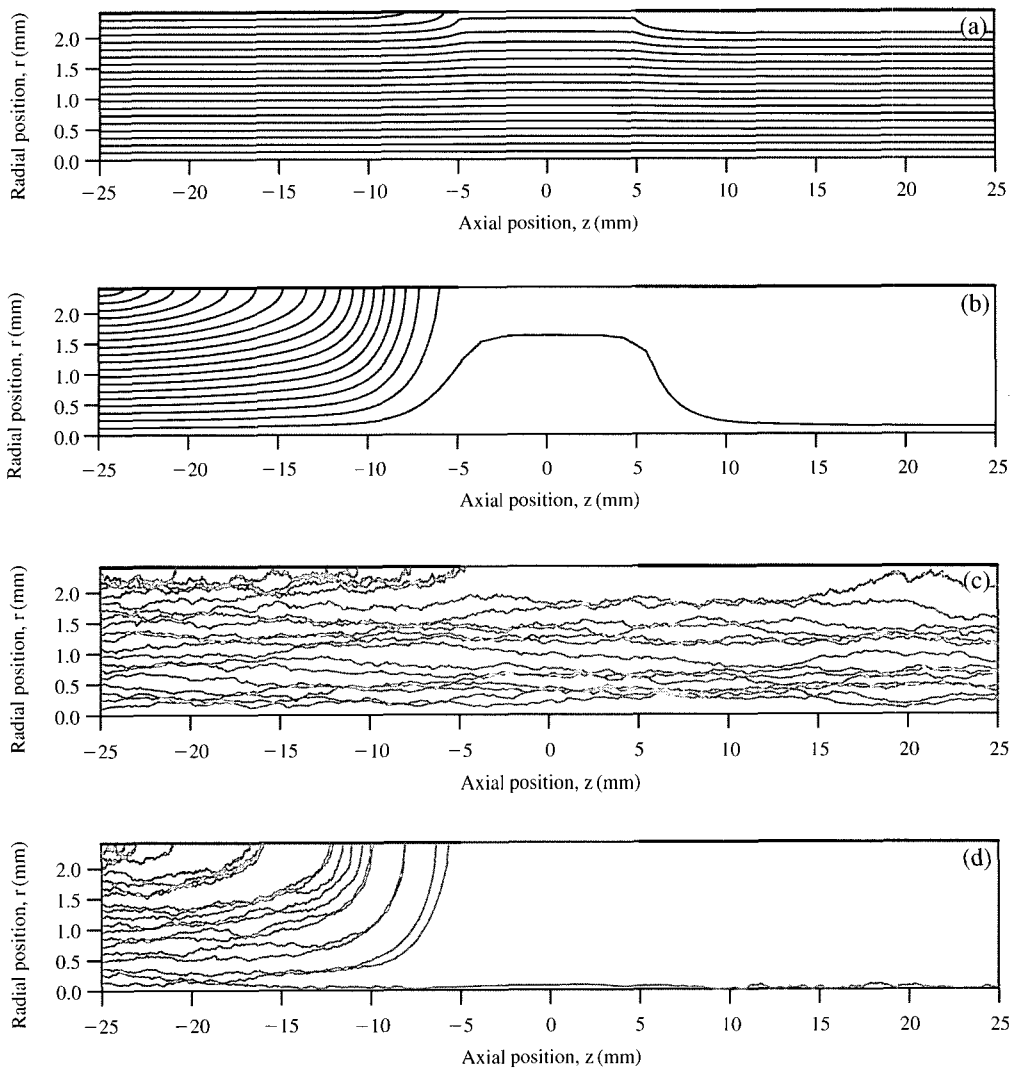

Fig. 5. Sample trajectories of charged particles passing the cylindrical tube having electrical voltage difference when d_p=2 nm; (a) V=10 V without diffusion, (b) V=5 kV without diffusion, (c) V=10 V with diffusion and (d) V=5 kV with diffusion.

applied voltage was changed to a different value (e.g., from V_1 to V_2), the distribution pattern did not change but the amplitude changed linearly, and the electrical strengths were also affected by the changed magnitude of the electrical potential.

Figure 5 shows sample trajectories of charged particles with diameter of 2 nm passing through the cylindrical tube with an electrical voltage difference with and without considering Brownian diffusion, when the applied voltage differences are 10 V and 5 kV. Charged particles enter from the aerosol inlet on the left side, move downstream, and are attracted by the electric force in the vicinity of the electrode edge. Some particles close to the cylinder wall are deposited, while particles near the radial centre line are weakly influenced by electric forces. After pass-

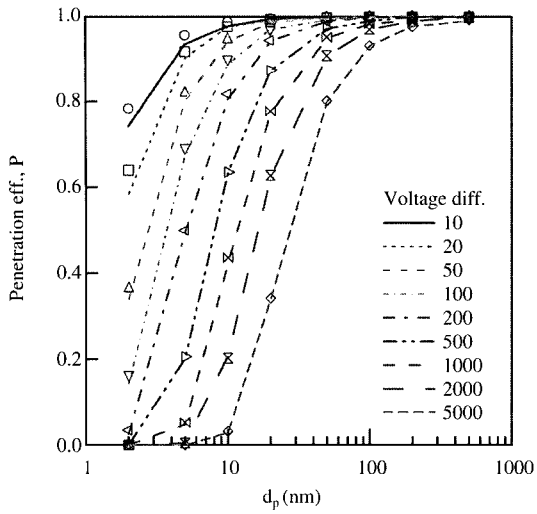

Fig. 6. Penetration efficiencies for various cases; symbols and lines represent penetration efficiencies with and without considering Brownian diffusion, respectively.

ing the centre of the insulator, the direction of electric force is reversed and the charged particles are repelled from the cylinder wall.

We calculated the penetration efficiency P for various particle diameters and applied voltages. The range of particle size and applied voltage used in the calculation were 2~500 nm and 0.01~5 kV, respectively. The ratio W/L of the insulator length to the total length was also changed from 0.1~0.4. In the numerical calculations, all particles were assumed to be spherical and singly charged with positive polarity. The dimensions of the cylindrical tube connection used for the numerical calculations were a half length of 25 mm and tube diameter of 0.19 inch, which is the inner diameter of Swagelok™ widely used in instruments for measuring aerosols.

Penetration efficiencies for the cases were obtained with and without considering Brownian diffusion, and shown in Figure 6. Penetration efficiency decreased as particle size increased and the voltage difference increased. There is a difference in the penetration efficiencies of cases with and without considering Brownian diffusion when the particles are smaller than about 20 nm.

5. DISCUSSION

5.1 Diffusion loss

As shown in Figure 5, the non-diffusing trajectory of particles close to the cylinder wall is directed towards the wall when the particles approach the electrical insulator and is directed away from the wall as the particles pass the insulator. The spatial distribution of particles is broadened by Brownian diffusion and it is known that it has a Gaussian distribution with a standard deviation σ given as

$$\sigma=\sqrt{2Dt} \tag{8}$$

where t is the elapsed time and D is particle diffusivity given by

$$D=\frac{k_b T C_C}{3\pi\eta d_p} \tag{9}$$

where k_b and T are the Boltzmann constant and the absolute temperature, respectively.

Friedlander (1977) determined the mass transfer coefficient for laminar pipe flow and overall penetration efficiency for a pipe of length L and diameter D_{tube} of

$$P_{p\text{-}d}=\exp\left[-6.46\left(\frac{L}{D_{tube}}Pe_p^{-1}\right)^{2/3}\right] \tag{10}$$

where $Pe_p=U_{avg}D_{tube}/D$ is the Peclet number for the pipe flow and the subscript p-d denotes the pure diffusion. Figure 7 shows a comparison of penetration efficiencies. P_{es} represents penetration efficiency considering electrostatic loss only and $P_{e\text{-}d}$ represents penetration efficiency with simultaneous consideration of electrostatic loss and diffusion loss. The products of P_{es} and $P_{p\text{-}d}$ are closer to $P_{e\text{-}d}$, but there is still a discrepancy, especially for cases of small particles and low applied voltages.

As Song and Dhaniyala (2007) noted, the spatial distribution of particle positions by Brownian diffusion under non-uniform external force fields preserves the Gaussian distribution with a standard deviation different from Eq. (8) and may even be skewed. The standard deviation of particle position distribution under a non-uniform external force field

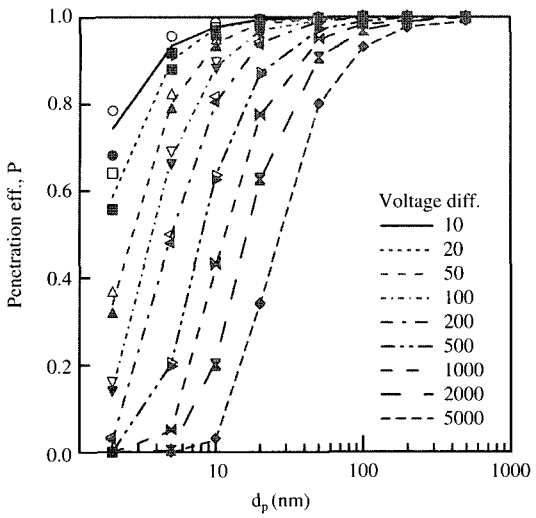

Fig. 7. Comparison of penetration efficiencies; Open symbols for P_{es}, lines for P_{e-d} and closed symbols for $P_{es} \cdot P_{p-d}$.

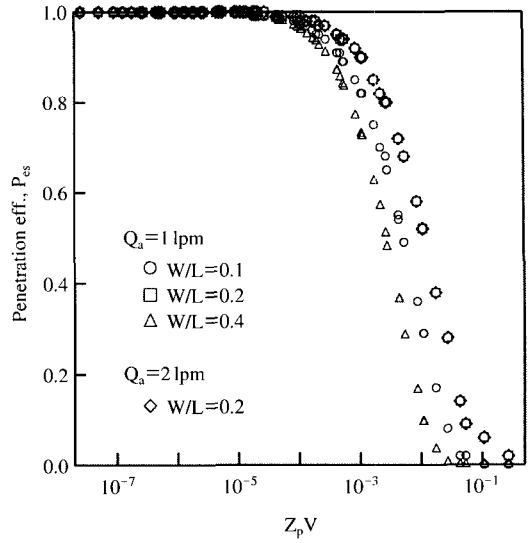

Fig. 8. Penetration efficiencies versus product of the applied voltage difference V and electrical mobility Z_p of particles.

depends on the form of non-uniformity in the force field. The local electric forces in the vicinity of edges of electrodes are not uniform; hence, there is a possibility that the difference in the penetration efficiency of cases with and without consideration of Brownian diffusion will differ from that of pure Brownian diffusion.

5.2 Electrode geometry

Since the electrostatic loss of charged particles is caused by radial electric forces, the amount of charged particles captured on the cylindrical tube wall can be characterized by the electrical migration velocity v_E to the wall. The electrical migration velocity is determined by electric force and electrical mobility Z_p of charged particles, given by

$$Z_p=\frac{neC_C}{3\pi\eta d_p} \tag{11}$$

where n and e are the number of elementary charges and the elementary electrical charge, respectively. Further, the electric strength is proportional to the voltage difference, so $Z_p \cdot V$ will be the key parameter when determining the amount of electrostatic losses. Figure 8 shows penetration efficiency as a function of $Z_p \cdot V$. The shape of the penetration efficiency curve is a so-called "S" curve and curves for various cases reside on a single curve, though there are some discrepancies.

If the length ratio W/L is changed, the absolute value of the electrical strength will also change, though the spatial shape of the electric forces is preserved. To investigate the effect of the length ratio, penetration efficiencies for cases of W/L=0.1, 0.2 and 0.4 were obtained, considering electrostatic loss only, and also shown in Figure 8. There is some discrepancy in penetration efficiency for the same $Z_p \cdot V$ value. For the case in which the flow rate is doubled with the same tube dimensions as when W/L=0.2, comparison shows no difference in penetration efficiencies.

A new non-dimensional parameter is introduced to generalize the penetration efficiency curve. Since the dimension of $Z_p \cdot V$ is [m^2/s], we selected a new parameter Es given as

$$Es=\frac{Z_pV}{U_{avg}W}=\frac{Z_pV}{Q_aW}\frac{\pi D_{tube}^2}{4} \tag{12}$$

Penetration efficiencies plotted over the new par-

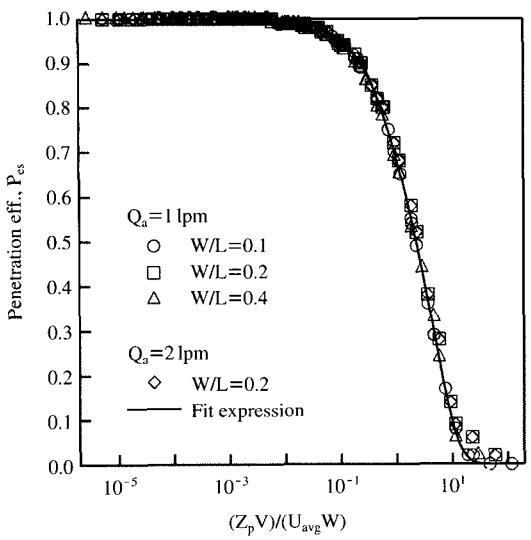

Fig. 9. Penetration efficiencies over a new non-dimensional parameter, Es.

ameter Es are shown in Figure 9 and all the penetration curves are located on a single curve. The fitted curve function as a form of exponential is obtained as

$$P_{es}=0.2\exp\left(-\frac{Es}{0.6324}\right)+0.8\exp\left(-\frac{Es}{4.7914}\right) \quad (13)$$

We should note that the penetration efficiency is obtained for the same tube length and tube diameter, so a more general expression for the penetration efficiency is needed to cover cases of different tube lengths or tube diameters.

6. CONCLUSIONS

We modelled a cylindrical tube connection that has a voltage difference and is separated electrically by an insulator, and investigated the penetration efficiency of charged particles passing through the connector tube. The penetration efficiency decreases as the particle size decreases and the applied voltage difference increases. From the comparison of penetration efficiencies for various length ratios of insulator to the total length, the penetration efficiency can be described as a function of the product of applied voltage and electrical mobility of charged particles. We also provided an explicit expression for penetration efficiencies as a function of a newly introduced non-dimensional parameter, Es.

ACKNOWLEDGEMENTS

"This work was supported by the Korea Research Foundation Grant (KRF-2004-003-D00157)."

REFERENCES

Allen, M.D. and O.G. Raabe (1982) Re-Evaluation of Millikan's Oil Drop Data for the Motion of Small Particles in Air. J. Aerosol Sci., 13, 537-547.

Bae, G.N., M.C. Kim, D.Y. Lim, K.C. Moon, and N.J. Baik (2003) Characteristics of urban aerosol number size distribution in Seoul during the winter season of 2001. J. KOSAE, 19(2), 167-177.

Chen, D.-R., D.Y.H. Pui, D. Hummes, H. Fissan, F.R. Quant, and G.J. Sem (1998) Design and evaluation of a nanometer aerosol differential mobility analyzer (Nano-DMA). J. Aerosol Sci., 29(5/6), 497-509.

Collins, D.R., D.R. Cocker, R.C. Flagan, and J.H. Seinfeld (2004) The scanning DMA transfer function. Aerosol Sci. Technol., 38, 833-850.

Donaldson, K., X.Y. Liu, and W. MacNee (1998) Ultrafine (nanometer) particle mediated lung injury. J. Aerosol Sci., 29, 553-560.

Ermak, D.L. and H. Buckholz (1980) Numerical integration of the Langevin equation: Monte Carlo simulation. J. Comp. Phys., 35, 169-182.

Friedlander, S.K. (1977) Smoke, Dust, and Haze. Wiley, New York, p. 77.

Jaques, P.A. and C.S. Kim (2000) Measurement of total lung deposition of inhaled ultrafine particles in healthy men and women. Inhalation Toxicology, 12, 715-731.

Keskinen, M., K. Pietarinen, and M. Lehtimaki (1992) Electrical low pressure impactor. J. Aerosol Sci., 4, 353-360.

Kim, Y.M. and K.H Ahn (2005) Monitoring of airborne fine particle using SMPS in Ansan area. J. KOSAE, 21(3), 295-301.

Kittelson, D.B. (1998) Engines and nanoparticles. J. Aerosol Sci., 29, 575-585.

Kousaka, Y., K. Okuyama, M. Adachi, and T. Mimura (1986) Effect of Brownian diffusion on electrical classification of ultrafine aerosol particles in differential mobility analyzer. J. Chem. Eng. Jpn., 19(5), 401-407.

Lee, J.W., H.S. Kim, and Y.I. Jeong (2006) Effects of particle measuring conditions on diesel nanoparticles distribution. J. KOSAE, 22(5), 653-660.

Myojo, T., S. Ikawa, H. Sakae, and N. Koyama (2001) A new long DMA and its performance for size-measurement of 1 μm Polystyrene latex particles. J. Jpn. Air Cleaning Assoc., 39, 34-41.

Oberdörster, G., J. Ferin, R. Gelein, S. Soderholm, and J. Finkelstein (1992) Role of the alveolar macrophage in lung injury: studies with ultrafine particles. Environmental Health Perspectives, 97, 193-199.

Oberdörster, G., R. Gelein, J. Ferin, and B. Weiss (1995) Association of particulate air pollution and acute mortality: involvement of ultrafine particles? Inhalation Toxicology, 71, 111-124.

Park, D.S., T.O. Kim, and D.S. Kim (2003) An analysis of characteristics of particulate matter exhausted from diesel locomotive engines. J. KOSAE, 19(2), 133-143.

Petäjä, T., G. Mordas, H. Manninen, P.P. Aalto, K. Hämeri, and M. Kulmala (2006) Detection efficiency of a water-based TSI condensation particle counter 3785. Aerosol Sci. Technol., 40(12), 1090-1097.

Schiller, C.F., J. Gebhart, J. Heder, G. Rudolf, and W. Stahlhofen (1986) Factors influencing total deposition of ultrafine aerosol particles in the human respiratory tract. J. Aerosol Sci., 17, 328-332.

Shimada, M., H.M. Lee, C.S. Kim, H. Koyama, T. Myojo, and K. Okuyama (2005) Development of an LDMA-FCE System for the Measurement of Submicron Aerosol Particles. J. Chem. Eng. Jpn., 38(1), 34-44.

Song, D.K., H. Chang, S.S. Kim, and K. Okuyama (2005) Numerical evaluation of the transfer function of a low pressure DMA by using the Langevin dynamic equation. Aerosol Sci. Technol., 39(8), 701-712.

Song, D.K. and S. Dhaniyala (2007) Change in distributions of particle positions by Brownian diffusion in a non-uniform external field. J. Aerosol Sci., 38(4), 444-454.

Song, D.K., H.M. Lee, H. Chang, S.S. Kim, M. Shimada, and K. Okuyama (2006) Performance evaluation of long differential mobility analyzer (LDMA) in measurements of nanoparticles. J. Aerosol Sci., 37(5), 598-615

Tu, K.W. and E.O. Knutson (1984) Total deposition of ultrafine hydrophobic and hygroscopic aerosols in the human respiratory system. Aerosol Sci. Technol., 3, 453-465.

Vincent, J.H. and C.F. Clement (2000) Ultrafine particles in workplace atmospheres. Phil. Trans. R. Soc. Lond. A, 358, 2673-2682.

Wang, J., R.C. Flagan, and J.H. Seinfeld (2002) Diffusional losses in particle sampling systems containing bends and elbows. J. Aerosol Sci., 33, 843-857.

Wichmann, H.-E. and A. Peters (2000) Epidemiological evidence of the effects of ultrafine particle exposure. Phil. Trans. R. Soc. Lond. A, 358, 2751-2769.

Wilson Jr, F.J., F.C. Hiller, J.D. Wilson, and R.C. Bone (1985) Quantitative deposition of ultrafine stable particles in the human respiratory tract. J. Appl. Physiol., 58, 223-229.

Woo, K.S., D.-R. Chen, D.Y.H. Pui, and P.H. McMurry (2001) Measurement of Atlanta aerosol size distributions: Observations of ultrafine particle events. Aerosol Sci. Technol., 34, 75-87.

Zhang, S.-H. and R.C. Flagan (1996) Resolution of the radial differential mobility analyzer for ultrafine particles. J. Aerosol Sci., 27(8), 1179-1200.